

Low Voltage High PVT Variation Tolerance Central Pattern Generators Design for a Biomimetic Micro Robot

ABSTRACT

This paper presents a low power circuit design of electronic central pattern generators (CPGs) of biomimetic robot which mimic the rhythm of lamprey based swimming pattern. The circuit has been designed using 65nm COMS Predictive Technology Model (PTM) at 0.8V supply. The design challenges of narrow voltage design margin and high sensitivity to parameter variation are addressed by circuit optimization technique as well as appropriate amplitude and time parameters' scaling. The electronic CPGs consist of electronic neurons and electronic synapses' interconnection, where the behaviors of the neuron and synapse adopt Hindmarsh-Rose (HR) neural model to replicate biological meaningful neurons and a first order chemical synapse model is utilized to achieve active synapses. Simulation results prove that the important properties of tonic bursting in both time domain and phase plane agree with the mathematical analysis. The electronic synapses are designed and optimized considering extensive device parameter variations to accommodate the low supply voltage requirement without sacrificing their accuracy. The simulation results validate the electronic CPGs performance at 0.8V supply voltage with parameter variation tolerance of 5% dissipating 3.28mW, which is acceptable for manufacture.

Categories and Subject Descriptors

B.7.1 [Integrated Circuits]: Types and Design Styles – Algorithms implemented in hardware

General Terms

Algorithms, Performance, Design.

Keywords

Electronic Neuron, Electronic synapse, Electronic CPGs.

1. INTRODUCTION

Biomimetic robotics is attracting the interest of growing number of robotics researchers worldwide. The advancements of robotics technologies have recently led to an increased interest towards biomimetic robotics as well in the scientific fields related to

Permission to make digital or hard copies of all or part of this work for personal or classroom use is granted without fee provided that copies are not made or distributed for profit or commercial advantage and that copies bear this notice and the full citation on the first page. To copy otherwise, or republish, to post on servers or to redistribute to lists, requires prior specific permission and/or a fee.

Conference '10, Month 1–2, 2010, City, State, Country.

Copyright 2010 ACM 1-58113-000-0/00/0010...\$10.00.

biology and to the study of living organisms. In fact, biomimetic robotics can represent a powerful tool today for experimental investigation of the sophisticated mechanisms and amazing sensory-motor performance that many living organisms show. One central topic is developing their movement control under unstructured operation environment. For underwater application, unexpected flow fluctuations and obstacles requires the biomimetic robots to have life-like reaction to the dynamic environments. Another design challenge lies on the isolated operation area and long working time, which requires the robots to have self-support energy and small body to minimize the power consumption. In order to meet these requirements, the improvement of the movement control needs to be low power and area economic. A number of digital biomimetic robot controlling schemes have been reported. However, the majority of them show poor performances in complicated environments due to inability to adapt to dynamic environments and their discrete-time responses. Digital circuit approaches turned out to be not realistic due to their size, power, and inadaptability to dynamic environments while analog circuits tend to be very well adaptive to the dynamic natural environments. Therefore, analog integrated circuit design for biomimetic control is suggested as a better way to achieve the goal [1]. However, power and chip area consumption remain as primary concern in analog approaches. To address the power and area issues, an advanced 65nm CMOS PTM [2] technology is employed in this paper with a supply voltage as low as 0.8V, which reduces the circuit area and power consumption significantly in comparison with the conventional 2V design in [1]. The proposed CPGs design in this paper is based on lamprey swimming pattern, which is more up-to-date and simplified than previous ones and results in dramatic decrease the complicity of the conventional CPGs in [1]. The proposed CPGs is implemented using aggressive amplitude and time scaling, low power circuit design technique, and parameters' optimization of the neuron model and circuits to overcome the limited voltage design margin. The parameter tolerance of 5% has been achieved by neuron parameter adjustment to meet the manufacture requirements.

This paper is organized as follows: Section II briefly introduces Cyberplasm micro-robot and CPGs. HR neuron model's mathematical analysis and circuit implementation are covered in Section III. Section IV presents the chemical synapse design and Section V provides the whole CPGs connection and simulation results. Concluding remarks of the paper are given in Section VI.

2. Cyberplasm Micro-robot

2.1 Description of Cyberplasm

The objective of Cyberplasm research is to create a novel, autonomous bio-hybrid micro-robot shown in Figure 1[3]. The robot uses synthetic muscles that are coordinated to underlie forward movement by articulating an anatomical tail. Synthetic sensors will be put in the head of the robot to receive locomotion direction signals due to its small area and dynamic sensitivity. The overall micro-robot is to be powered by a microbial fuel cell integrated into the robot body. The entire system will be tied together with an analog implementation of a biologically realistic nervous system. Biomimetic electronic CPGs coordinate the output muscles to create a rhythmic swimming pattern. The movements signal is transferred to muscles by organic LED grown over an on a Kapton substrate, because the synthetic muscles are sensitive to blue light. Finally, the robot will be covered by certain hull.

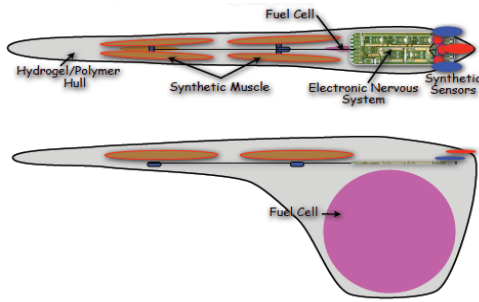


Figure 1 Diagram of the proposed Cyberplasm [3].

2.2 Central Pattern Generators

Central pattern generators imitate neural and synaptic networks that produce rhythmic patterned outputs without sensory feedback or central input [4]. CPGs are regarded as the origin of the most rhythmic motor patterns like walking swimming and breathing. Some invertebrates contained the simplest CPGs network can be studied and used in robotic movements design.

In the study of lamprey based swimming pattern generators, results reveal that the two CPGs in the same level on the two sides usually generate out-of-phase oscillation by reciprocal inhibitory connections, while the other two CPGs on the same side exhibit a homogeneous oscillation with a period varying phase delay [5]. Figure 2 depicts a simplified swimming pattern generator layout [6]. Although the actual swimming pattern generator can be much more complicated, it gives the biological meaning to the robot movements. *Lseg1*, *Lseg2*, *Rseg1* and *Rseg2* are four neurons and they are inhibited (shown as bubble at the inputs in Figure 2) by the oscillator. From the head to tail, the phase delay propagates the motion down the spine of the robot. There is an external control signal from sensors that controls speed-up or slow-down the neuron spiking. The control signal is not shown in this diagram.

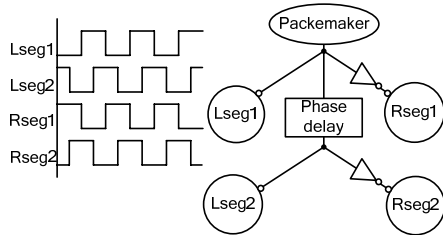


Figure 2 The rhythm pattern for the proposed swimming pattern generator [6].

3. Electronic Neuron Design

3.1 Hindermash Rose Neuron

It is obvious that neuron is a core element in CPGs. There are a number of neuron models that can be used for hardware realization. Reference [7] discusses the applicability and biological plausibility of various neuron models. Every neuron model has different properties. However, the most important property for the proposed biomimetic neuron design is tonic bursting for swimming rhythm. Therefore, the ‘‘Hindmarsh-Rose’’ neural model is chosen in our research since it fires a tonic bursting and provides the biological meaning of the real neuron’s membrane potential. Moreover, the model has more advantages in hardware realization because its behavior is described in lower order of equations and the frequency of the burst signal is accurately controlled by the input variable I . The three dimensional HR neuron model is written as [8]:

$$\frac{dx}{dt} = ay + bx^2 - cx^3 - dz + I \quad (1)$$

$$\frac{dy}{dt} = e - fx^2 - y \quad (2)$$

$$\frac{dz}{dt} = \mu(S(x+h) - z) \quad (3)$$

Where x is membrane potential, y is recovery current, z is adaptation current, I is applied current, and h is the leftmost equilibrium point of the neuron model without adaptation. The initial conditions for state variables (x_0, y_0, z_0) are (0, 0, 0). The typical coefficients are $a=1, b=3, c=1, d=0.99, e=1.01, f=5.0128, \mu=0.0021, S=3.966, h=1.605, I=[0, 3.024]$.

3.2 Mathematic Analysis of HR Model

According to the analysis in [8], by setting the z variable to zero, the HR neuron model is reduced to two differential equations with two unknowns. By setting the right half of equation (1) and (2) to zero, phase plane equations (4) and (5) can be obtained to reveal the spiking condition of this model. As shown in Figure 3, different graph of equations (4) and (5) can be plotted with different I . It is observed that increasing I lowers the curve of equation (4) causing the stable points to merge together and then vanish. This drives the system into an unstable region and limit cycle, causing output spiking [9], which is the exact property of tonic spiking.

$$y = \frac{1}{a}(cx^3 - bx^2 - I) \quad (4)$$

$$y = e - fx^2 \quad (5)$$

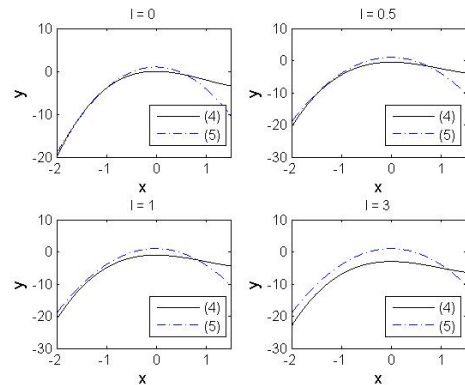


Figure 3 Graphs for the equation (4) and (5) with different I .

Tonic bursting fires periodic bursts of spikes when activated, and it often remains silent until activated. The z variable in the HR

equations controls this bursting mode in the three dimensional HR model. As the input increases, the stable equilibrium points vanish which causes a limit cycle as shown in Figure 3. Because z is the integration of variable x , each spike adds value to the variable z , which in turn raises the curve (4) in Figure 3. This lifting of the curve (4) counteracts the lowering effect of the input I . This action causes the output spikes to slow down as time goes by, then finally output spikes ceases. The system should return to the silent state. Because the variable x goes low, the variable z in turn falls allowing the system to be activated again and the spiking resumes itself.

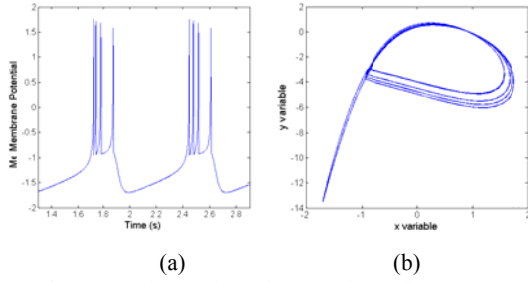


Figure 4 Matlab simulation of three dimensional HR model when $I=1.5$: (a) the x variable, (b) the phase plane of x and y .

Figure 4 shows the output of the three dimensional HR equations. Figure 4(a) represents the time domain tonic bursting of x variable. It is observed that x can burst for a time and silent for another time and present a periodic occurrence. The phase plane analysis is shown in Figure 4(b). Besides the unsymmetrical circle representing the bursting, the phase plane has a tail that stands for the silent period seen between bursts.

3.3 Circuit Implementation of HR neuron

The integrated circuit of the HR neuron has been designed using 65nm CMOS technology based on the HR neuron model and the research introduced in [10] as shown in Figure 6. By taking integration on both sides of HR neuron model, the circuit is created with analog integrators in voltage mode. Integrators are more stable than differentiator in circuit aspect, since the former has no steady state error. Although the variables in HR neuron model have current representation, the circuit design becomes less complicated when designed in voltage mode. In order to meet the requirements of 0.8V supply rail and reduce passive components' area on chip, both time and amplitude scaling have been employed, and the detailed information can be found in [10]. Scaled variables (x, y, z) are denoted by (X, Y, Z). The parameter tolerance of 5% is possible to achieve at 0.8V supply voltage by lowering the value of the ratios between R_4, R_5 and R_{x2} so that the curve separation in Figure 3 is controlled and maintained with relative easiness.

Figure 6 shows the circuit simulation results. Figure 6(a) includes a segment of variable X 's time domain tonic bursting, where it demonstrates the correct tonic bursting operation; it bursts for a period and it is silent for a period. The bursting width and silence width is modulated by input L in Figure 5, which has the same meaning as I . However, L is the scaled version of I (I is between 0 and 3 while L is between 0.55 and 0.8). Figure 6(b) is the corresponding phase plane of Y with respect to X . It has almost the same shape as Figure 4(b) but with more circles. That is because the loose circles are the starting region for the real circuits to reach the steady state and the dense circles represent longer bursting in Figure 6. (a). From the comparison of Figure 4 and

Figure 6, it can be concluded that HR neuron model has been successfully mapped to and implemented in integrated circuits.

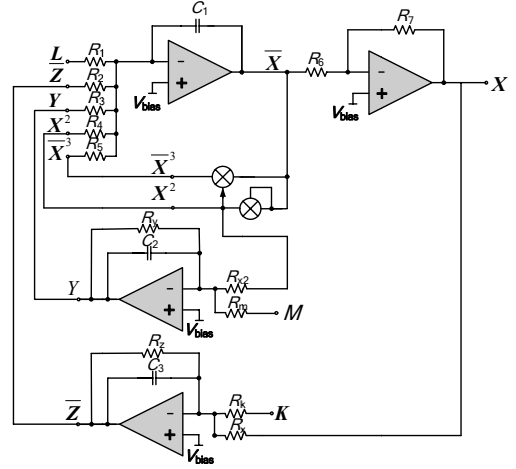


Figure 5 65 nm electronic neuron based on HR neuron model.

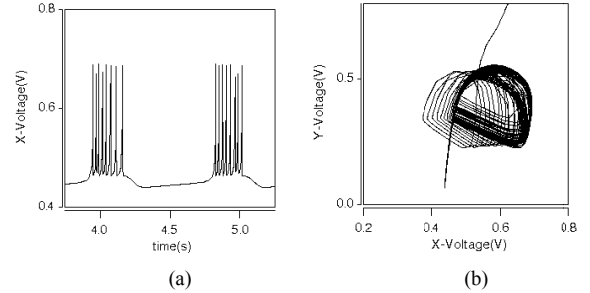


Figure 6 Electronic HR neuron simulation results when $L=0.6$: (a) X tonic bursting, (b) Y/X phase plane.

4. Electronic Synapse Design

4.1 Chemical Synapse Model

The synapse supplies the current to reshape the membrane potential of multiple electronic neurons. The bursting will be either synchronous (excitatory coupling) with depolarizing current injection or asynchronous (inhibitory coupling) with hyperpolarizing current injection. The chemical synapse model is given in [11] as:

$$I = gS(t)(V_{rev} - V_{post})$$

$$\frac{dS(t)}{dt} = \frac{S_{\infty} - S(t)}{\tau_S(1 - S_{\infty})}$$

$$S_{\infty} = \tanh\left(\frac{V_{pre} - V_{th}}{V_{slope}}\right)$$
(6)

Where g is the maximal synaptic conductance, $S(t)$ is instantaneous synaptic activation, S_{∞} is the steady-state synaptic activation, V_{rev} is the synaptic reversal potential, V_{pre} is presynaptic voltage, V_{post} is the postsynaptic voltage, V_{th} is the synaptic threshold for transmitter release, V_{slope} is the synaptic slope voltage, and τ_S is the synaptic time constant.

4.2 Circuit Implementation of Synapse

65nm VLSI implementation of synapse has been introduced in [10] as shown in Figure 7. It is the hardware implementation of the three equations in equation (6). The differential expression is achieved by integration, and the hyperbolic tangent function is

approximated to expression $-x$ using Taylor Series taking advantage of the small signal amplitude in this 0.8V supply system. The multiplication in the model is replaced by a transfer gate which produces the same results, because the amplitude swing of the multiplication does meet the high common mode input range requirement of a normal multiplier.

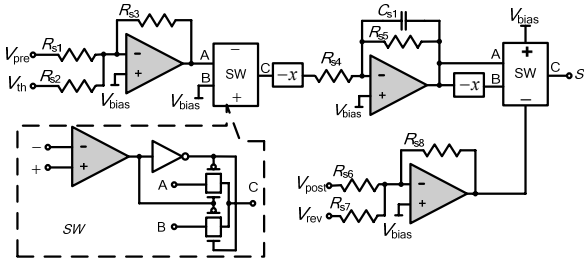


Figure 7 65 nm electronic synapse circuit.

In the excitatory state, the synapse produces signals above the virtual ground to modulate two independent neurons to oscillate at the same time. In contrast, the two independent neurons will oscillate out-of-phase when the synapse signals are below the virtual ground in inhibitory state. The coupling strength can be tuned by the amplitude of synapse output. Therefore, a phase delay between the two neurons can be achieved by weak excitatory coupling between two neurons, which is done by the “Weak Excitatory” block in Figure 8. This coupling mechanism has been verified and published in [10].

5. Electronic CPGs Design

The complete electronic CPGs block diagram is shown in Figure 8. In order to accomplish the swimming pattern generator in Figure 2, neurons *Lseg1* and *Rseg1* are required to burst out-of-phase and so are *Lseg2* and *Rseg2*. At the same time, neurons on the same side, that is (*Lseg1*, *Lseg2*) and (*Rseg1*, *Rseg2*), have in-phase burst. Therefore, *Lseg1* and *Rseg1* are coupled with strong inhibitory synapses, and neurons on each side are coupled with weak excitatory synapse. The simulation results in Figure 9 agree with the desired theoretical output in Figure 2.

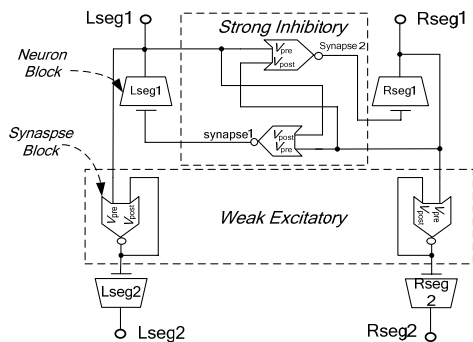


Figure 8 65 nm electronic CPGs.

6. Conclusion

A novel scheme of CPGs, imitating a lamprey swimming pattern, is proposed and designed to control the Cyberplasm’s movement of biomimetic robot in this paper. The CPGs are comprised of HR model based electronic neuron and first order chemical model based electronic synapse. Simulation results verify that the proposed CPGs behave as expected at 0.8V supply voltage with 3.28mW power dissipation. The system also exhibits a parameter

variation tolerance of 5%, which is acceptable for manufacturability. These advantages of the proposed CPGs design including low power, high PVT tolerance, and compact scheme meet the requirements of the biomimetic micro robot design requirements for Cyberplasm.

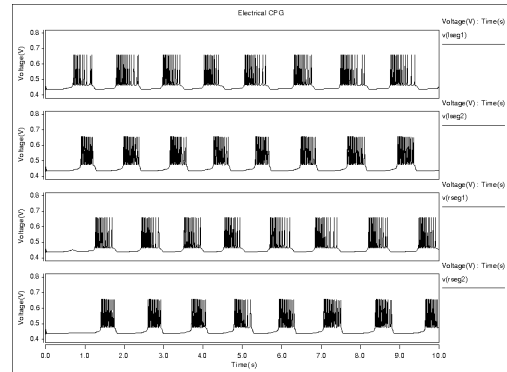


Figure 9 Simulation result of electronic CPGs.

7. REFERENCES

- [1] Nanoscale Integration and Modeling (NIMO) group, S. 2006. 65 nm BSIM4 model card for bulk CMOS: V1.0. Technical file Arizona State University.
- [2] J. Ayers, etc. AI, OL. 2009. <http://www.cyberplasm.net/>
- [3] J. Lee, Y. J. Lee, K. Kim, Y. B. Kim, and J. Ayers, J. .2007. Low power CMOS adaptive electronic central pattern generator design for a biomimetic robot. In *Neuroncomputing*, vol.71, pp. 284-296.
- [4] Hooper, Scott, M. 1999. Central pattern generators. *Encyclopedia of Life Sciences. John Wiley & Sons.* DOI:10.1038/npg.els.0000032.
- [5] A. Westphal, N. Rulkov, J. Ayers, etc.al, J. 2010. Controlling a lamprey-based robot with electronic nervous system. In *Smart Structures and Materials*. In press.
- [6] D. debolt, Y. B. Kim, and J. Ayers, C. 2011. Scaling issues for VLSI implementations of biologically accurate neurons and central pattern generators, In *2011 IEEE International SoC Design Conference (ISOC 2011)*.
- [7] E. Izhikevich, J. 2004. Which model to use for cortical spiking neurons? In *Neural Networks, IEEE Transactions on*, vol. 15, no. 5, pp. 1063-1070.
- [8] J.L.Hindmarsh and R. M. Rose, J. 1984. A model of neuronal bursting using three coupled first order differential equations, *Proc. of the Royal Society of London*, pp.87-102.
- [9] L. Merlat, N. Silvestre, and J. Merckle, C. 1996. A Hindmarsh and Rose based electronic burster. In *Proceedings of the 5th International Conference on Microelectronic for Neural Networks and Fuzzy Systems*.
- [10] J. Lu, Y. B. Kim, and J. Ayers, C. 2011. A low power 65 nm CMOS electronic neuron and synapse design for biomeimetic micro-robot. *IEEE International Midwest Symposium on Circuits and Systems (MWSCAS)*, Seoul, South Korea, Tp1B1(01-1099).
- [11] R. D. Pinto, etc.al, J. 2000. Synchrononus behavior of two coupled electronic neurons. *Physical Review E*, vlo.62, no.2, pp171-18.